PERGAMON

International Journal of Solids and Structures 39 (2002) 3797–3809

INTERNATIONAL JOURNAL OF SOLIDS and STRUCTURES

www.elsevier.com/locate/ijsolstr

Phase transformation in superelastic NiTi polycrystalline micro-tubes under tension and torsion—from localization to homogeneous deformation

Qing-Ping Sun *, Zhi-Qi Li

Department of Mechanical Engineering, The Hong Kong University of Science and Technology, Clear Water Bay, Kowloon, Hong Kong SAR, PR China

Abstract

Recent tension–torsion test results on nano-grained NiTi shape memory alloy micro-tubes are reported in this paper. It is discovered that: (1) during uniaxial tensile loading, the stress-induced transformation in the micro-tubes is realized by the initiation and growth of a macroscopic spiral martensite band with a quite sharp austenite–martensite (A–M) interface; (2) during loading by torsion (pure shear), the stress–strain curve exhibits monotonic hardening, the stress-induced transformation is axially homogeneous throughout the whole tube and the transformation strain is much smaller than that under tension; (3) under tension–torsion combined loading with an increasing shear/tension stress ratio, there is a gradual change in the deformation mode from localization and propagation (under pure tension) to the homogeneous deformation (under pure shear). The tube surface morphology observation indicates that, during this gradual change, the A–M interface thickness increases as its evolution is recorded. The test results demonstrate that there is a strong anisotropy and loading path dependence of the tube responses in both kinematics and kinetics. Possible underlying physical mechanisms are analyzed and implications for future theoretical modelling are also discussed.

Keywords: Phase transformation; NiTi shape memory alloy micro-tubes; Tension/torsion test; Material instability; Thickness of A–M interface

1. Introduction

Applications of shape memory alloys (SMAs) in the medical industry are multiplying rapidly. NiTi polycrystalline SMAs, due to their unique superelastic properties and biocompatibility, have been successfully used as components of medical devices in recent years. An outstanding example is of their use in minimal access surgery and less invasive operations as guidewires, guidetubes and stents. The high flexibility, large recoverable deformation, good fatigue life and outstanding superelastic behavior at or around body temperature of NiTi superelastic tubes and wires make it possible to minimize the size of critical

* Corresponding author. Tel.: +852-2358-8655; fax: +852-2358-1543.
E-mail address: meqpsun@ust.hk (Q.-P. Sun).

0020-7683/02/$ - see front matter
PII: S0020-7683(02)00182-8

medical devices and to perform functions that would be impossible with other materials. High mechanical reliability (such as kink resistance) and controllability of the deformation of the devices (via stress/temperature-induced phase transitions) are two critical requirements of very long and small-diameter surgical instruments (allowing push/pull/twist manipulations) (Duerig, 1995; Pelton et al., 1997). These requirements are dependent upon the constitutive behavior of the material under complex loading conditions. Experimental investigation on NiTi micro-tube materials has been conducted in recent years and some preliminary results have been obtained (see Pelton et al., 1997; Sun et al., 2000; Li and Sun, 2002).

Fundamental mechanics studies on the behavior and modelling of bulk superelastic NiTi wires and strips have attracted a lot of research attention in the past decade (for example see Abeyaratne and Knowles, 1990, 1993; Shaw and Kyriakides, 1995, 1997, among many others). In recent years, the effect of texture and microstructure anisotropy on the constitutive behavior of SMAs has become an issue of interest and has been investigated by many researchers (for example, the work of Thamburaja and Anand (2001), Shu and Bhattacharya (1998), Miyazaki et al. (2000), Gall and Sehitoglu (1999), Patoor et al. (2001), Sittner and Novak (2000), Liu et al. (1999) and Song et al. (2000a,b)). The micro-tubes are typically obtained by drawing process during which severe plastic deformation happened and a strong crystalline texture may develop in the tubes. Therefore the micro-tube samples make it possible to combine biaxial test with material anisotropy test. Experimental investigation to understand the fundamental mechanics of nano-grained NiTi micro-tube materials has not yet been reported. Test data for critical comparisons with exiting theoretical modelling are lacking.

This paper reports on an experimental study of the constitutive behavior of polycrystalline NiTi micro-tube material under tension, torsion and tension/torsion combined loadings. The main objective of this work is to reveal the effect of external stress states as well as internal microstructures on the macroscopic behavior of the material during phase transformation. The specimen preparation and experimental procedures are described in Section 2 and the results of uniaxial tension are briefly reported in Section 3. In Section 4, the results under pure torsion and torsion/tension combined loading tests are reported. Macroscopic nominal stress–strain curves under different tension/torsion loading ratios are measured and presented. Quantitative surface morphology observations are also reported on the material under different loading conditions, especially in regards to variations in the austenite–martensite (A–M) interface thickness during the loading. The results are discussed in Section 5 in which issues regarding the underlying mechanisms and the theoretical modelling of the observed phenomena are addressed.

2. Experimental procedures

2.1. Material

The micro-tubes are commercially available (Shape Memory Application, Inc., USA) polycrystalline NiTi with grain sizes of 30–50 nm. Micro-tubes of two sizes are used in the test: one with an outer diameter of 1.12 mm and other of 1.5 mm. The usual thickness/diameter (t/D) ratios for both tubes are 10%. In the tests of each tube diameter, all specimens are cut from a single tube in order to reduce fluctuations in material properties. The composition (provided by the manufacturer) and the transition temperatures of the materials (measured by a differential scanning calorimeter, DSC) are shown in Table 1. At room temperature (23 °C), the superelastic behavior of the material is guaranteed. During loading, austenite loses its stability and stress-induced martensite begins to form. During unloading, the stress-induced martensite becomes unstable and transforms back to austenite.

Fig. 1(a) shows schematically the mechanical cold-drawing process of NiTi micro-tubes. Tubes were drawn through dies using a guide bar to keep them straight and to give the final inner diameter. The outer diameter and thickness of the tubes are thus reduced and significant plastic deformation takes place. During

Table 1
Composition (wt.%) and transition temperatures (°C) of the tube materials

	Ni (%)	Ti (%)	A_s (°C)	A_f (°C)	M_s (°C)	M_f (°C)
1.12 mm tube	51	49	−2.69	22.4	−56.3	−77.6
1.5 mm tube	56	44	−3.26	17.4	−54.2	−67.6

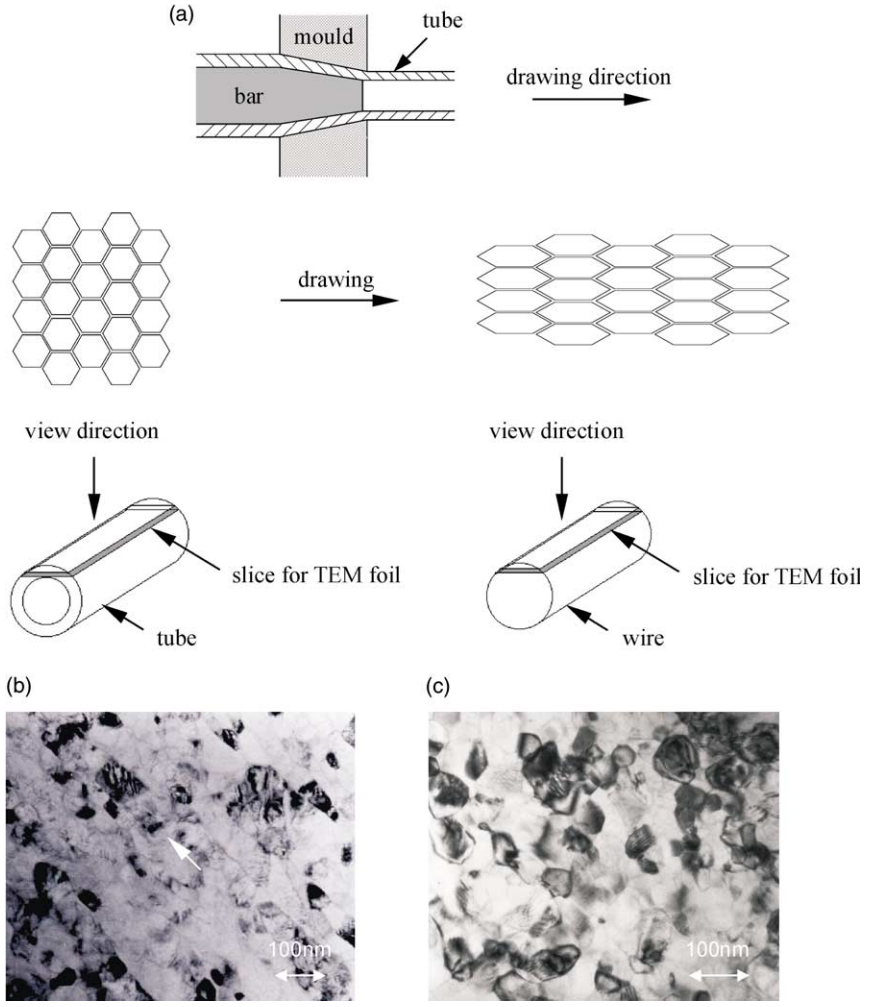

Fig. 1. (a) Schematic illustration of drawing process, (b) TEM picture of grain size of the tube (arrow shows the drawing direction) and (c) TEM picture of grain size of the wire (1.3 mm diameter) for comparison.

the drawing process, strong crystalline texture develops due to the rotation of the slip systems in the grains. To observe the microstructure of the material, a slice is cut along the axis direction of the tube. Fig. 1(b) shows a typical microstructure of the tube (grain sizes about 50–100 nm) by transmission electron microscopy (TEM). Fig. 1(c) is the TEM photo of a much less deformed drawn wire (1.3 mm diameter) for comparison. It is seen that there exists a strong texture in the tubes because of the severe plastic deformation during cold drawing. This contributes to significant anisotropy in the transformation behaviors between tension and torsion as shown in the following sections.

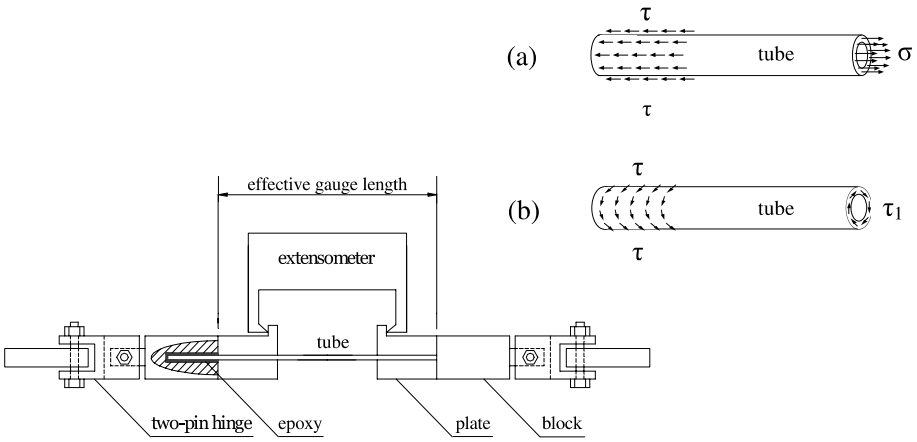

Fig. 2. The grips and the way to load the tube under (a) pure tension and (b) pure torsion.

2.2. Experiment set-up

(i) Uniaxial tension test. The experiments were conducted at room temperature (23 °C) in a standard testing machine (Sintech 10D with a 1 KN load cell) under displacement control. To clamp the tube for the tension and torsion tests and to eliminate the stress concentration in the clamped area, a special grip for thin-walled micro-tubes was designed as shown in Fig. 2(a). The blocks on which the tubes are adhered are connected to the test machine by two two-pin hinge connectors. This type of grip, which transfers a concentrated force at the end of cylinder into a uniform axial shear stress on the tube surface at the two ends, is very effective in removing the bending and torsion caused by the clamp's eccentricity. The tubes are bonded to the block by an epoxy (plastic welding system, no. 47809, shear strength at room temperature 3500 psi). The bonded length of each tube is 20 mm at each end. An extensometer is used to measure the tube elongation and nominal strain. In order to hold the extensometer, two additional plates are fixed to the blocks by screws. In this way, the effective gauge length is 52 mm (Fig. 2).

(ii) Torsion and tension/torsion tests. The responses of the tubes under torsion and tension/torsion were measured at room temperature (23 °C) in a standard testing machine together with a specially designed torsion loading device. The clamp of the tube for the torsion (Fig. 2(b)) and the tension/torsion tests is similar to that for the uniaxial tension test described above (Fig. 2(a)). The blocks on which the tubes are adhered are connected to the test machine by two two-pin hinge connectors. This type of grip transfers both concentrated force and torque at the end of cylinder into quite uniform tensile and shear stresses over the tubes' cross-sections in the measured section of the tube. The tubes are fixed on the block with a strong epoxy and the bonded length of the tubes is 20 mm at each end. The angle of rotation of the tubes is measured and used to calculate the average shear strain.

3. Test results under uniaxial tension

In this section we briefly report the results from the uniaxial tension tests (for more detailed descriptions and analyses, see Li and Sun (2002)). Fig. 3(a) shows a typical measured nominal stress–strain curve of a micro-tube under tension. To observe the nucleation and propagation of a macroscopic martensite band in the micro-tubes, the tubes were coated with a very thin brittle layer of rosin (with a break strain of 2%) and loaded under an optical microscope. The photo of the surface morphology of the tube (Fig. 3(b)) reveals

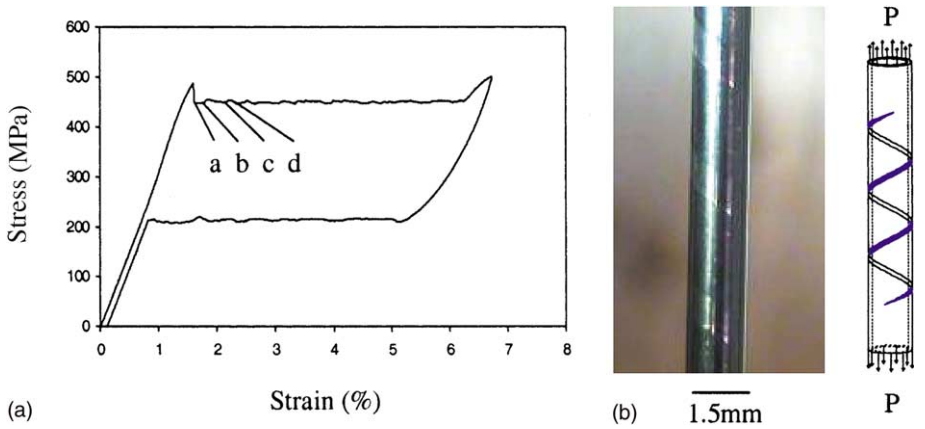

Fig. 3. (a) The nominal tensile stress–strain curve of micro-tube, (b) photo and schematic illustration of the surface morphology of the tube.

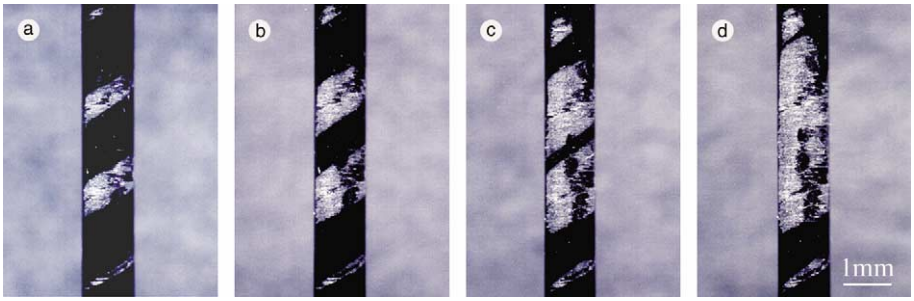

Fig. 4. The nucleation and growth of martensite band (white color) in micro-tube: (a) the nucleation of a spiral shaped martensite band, (b, c) the growth of martensite band, (d) merge into a cylindrical band.

that the initial band (white color in Fig. 4) is in a spiral shape. The spiral inclines at about 61° to the axis of loading. The tube surface morphologies at different stages of loading are shown in Fig. 4 where the corresponding positions on the nominal stress–strain curve are marked in Fig. 3(a). The length of the martensite band is $L_a = 13.1$ mm and the width at the middle portion of the band is $W_a = 0.76$ mm at point a (immediately after the martensite band nucleates, see Fig. 4(a)). The corresponding stress drop is 42 MPa (Fig. 3(a)). During the subsequent loading after the initial nucleation, the stress remains almost constant and the martensite band grows gradually in its length and width. At point b of Fig. 3(a), the width and length of the band increases to $W_b = 1.1$ mm and $L_b = 13.8$ mm (Fig. 4(b)). There is a clear interface between the martensite and the austenite domains (here referred to as the A–M interface). With further increase in tube elongation, the middle portion of the band continues to widen with the two A–M interfaces remaining almost parallel to each other. Finally, the band begins to merge at point d (Fig. 3(a) and Fig. 4(d)). Also, the length of the band reaches its maximum (about 16 mm). After point d, the length of the front (interface) decreases rapidly due to the self-coalescence of the band and, as a result, the propagation speed of the front increases rapidly. Fig. 4 shows that the A–M interface in the micro-tube is quite sharp at different stages of loading. Fig. 5 shows the measured tube surface morphology profile across a martensite band along the axial direction of the tube by using the surface profile system (Model α-step 2000 (Tencor)). There is a very rapid depth change or macroscopic strain variation (gradient) across the A–M interface.

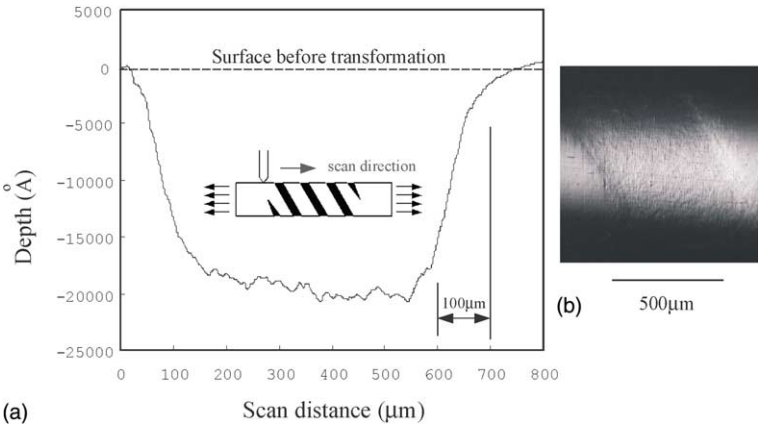

Fig. 5. The measured surface morphology profile across a martensite band and its two A–M interfaces and photo of the martensite band (1.5 mm tube).

Fig. 5 also shows that the interface thickness is about 100 μm. This value is of the same order as the thickness of the tube (150 μm). More detailed observation on the interface thickness morphology of the tube under torsion and tension–torsion is described in the following sections.

4. Test results under pure torsion and tension–torsion combined loading

4.1. Deformation of micro-tube under pure torsion

In strong contrast with the tension test, the tubes behave very differently under torsion. Fig. 6 shows the measured stress–strain curve of the micro-tube under pure torsion. The shear stress–shear strain curve is monotonic, which means that the macroscopic deformation of the tube is stable. Both surface morphology analysis and optical microscope observation indicate that the deformation is homogeneous across the whole

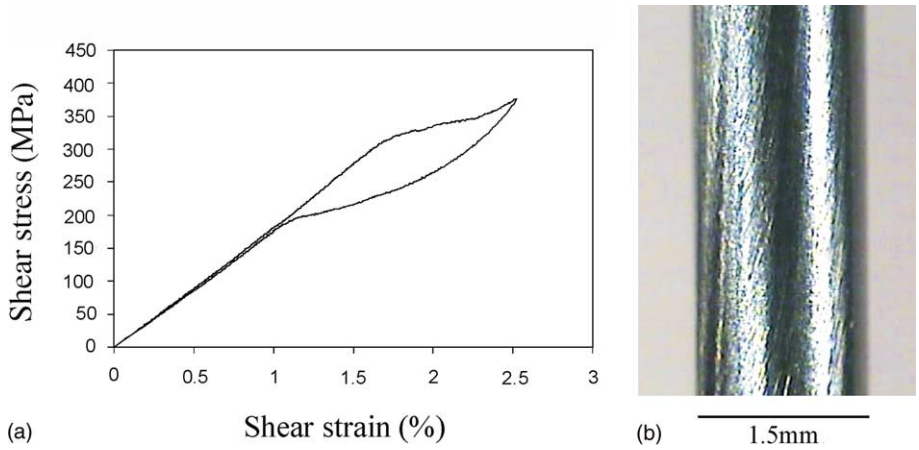

Fig. 6. (a) The stress–strain curve of micro-tube under pure torsion, (b) the surface morphology of tube.

tube as shown in the photo in Fig. 6(b) (in fact it is axially homogeneous since there is a shear strain gradient through the tube wall thickness). No macroscopic helical (torsional) buckling is observed during the test, which indicates that the tube wall thickness is not thin enough to buckle mechanically before transformation.

Another unusual aspect of the pure torsional behavior is that the maximum transformation shear strain is only about 0.7% (Fig. 6(a)), which is not only much smaller than that in uniaxial tension (≈5% in Fig. 3(a)) but also much smaller than the measured transformation shear strain of a previously reported biaxial test on a bulk NiTi tube sample (wall-thickness 2 mm and grain size 40 μm, see Lim and McDowell, 1999). Furthermore, the initial transformation stress under pure shear did not fall on the same Von-Mises circle with that under tension (see Fig. 9). Even in the linear elastic stage of the loading (before transformation), the measured values of Young's modulus, E, of austenite (≈30 GPa from tension in Fig. 3(a)) and the shear modulus, G, of austenite (≈18 GPa from torsion in Fig. 6(a)) do not satisfy the isotropic relationship ($G = E/2(1 + v)$).

4.2. Deformation of micro-tube under tension/torsion combined loading

Two types of loading paths are used in the biaxial tests.

Type I loading: This is a series of tensile test of the tube under different constant applied shear stresses that are below the initial transformation stress under pure shear. The purposes of this type of loading are: (1) to check the effect of applied shear stress on the tensile response as well as on the changes in the morphology of the tube surface; (2) to obtain the initial transformation stress locus (see Section 4.3) under the biaxial stress state. The tensile stress–tensile strain curves at different given shear stresses (constant values of applied torque) are shown in Fig. 7. It is seen that, at relatively low levels of shear stress, the responses of the tube in the axial direction are unstable as demonstrated by the small stress peak (load drop) and the subsequent stress plateau in the tensile stress–tensile strain curves. The tube surface morphology observation indicates that the transformation is still realized by the initiation and growth of a spiral martensite band with a quite sharp A–M interface and with the same orientation as that in Figs. 3 and 4 (uniaxial tension). No variation in band orientation with the applied shear stress is observed at these relative low shear stresses. With further increase in the shear stress level, the above localized deformation

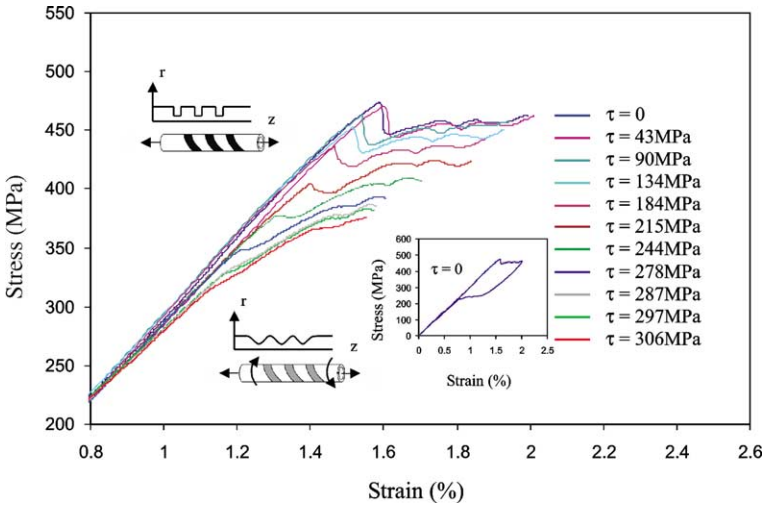

Fig. 7. Tensile stress–tensile strain curves at different given shear stresses.

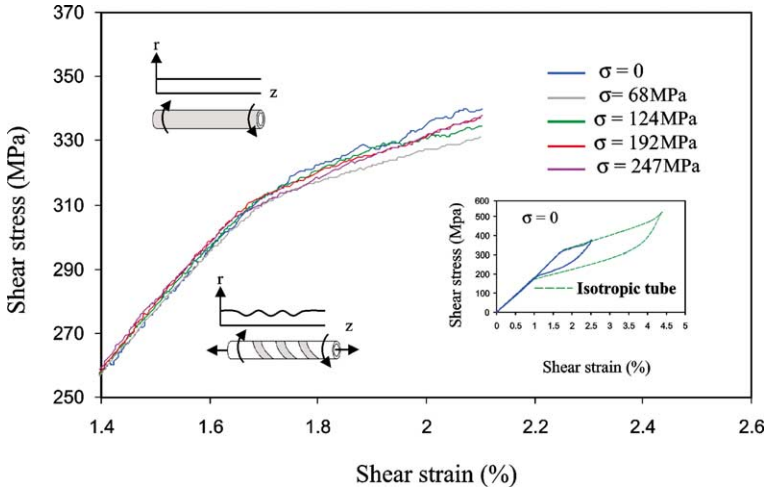

Fig. 8. Shear stress–shear strain curves at different given tensile stresses.

mode becomes less and less dominant and finally the stress–strain curves become monotonically hardened as shown in Fig. 7. The transformation strain distribution over the tube tends to be more homogeneous and band morphology with a diffusive A–M interface can be observed on the tube surface. Eventually, no band can be observed on the tube surface and deformation becomes homogeneous along the axial direction.

Type II loading: This is a series of torsion tests of the tubes under different values of constant axial tensile stress that is less than the uniaxial transformation stress under pure tension. The corresponding shear stress–shear strain curves at different given tensile stresses (constant values of applied axial force) are shown in Fig. 8. It is seen that there are only small differences among the shear stress–shear strain curves. At relatively lower levels of tensile stress, the responses of the tube under shear are stable (with homogeneous deformation and monotonic hardening shear stress–shear strain curves). However, at relatively higher levels of tensile stress, though the responses of the tube in shear are still stable with homogeneous shear deformation, the gradual increasing wavy morphology observed on the tube surface indicates that there exists an inhomogeneity in axial deformation.

4.3. Initial transformation stress locus and transfer of deformation mode

The initial stress locus at the start of the transformation is constructed from the data of Type I and Type II loadings and is plotted in Fig. 9. The Von-Mises circle is also plotted for comparison. It is important to notice the stress paths (order of loading) used to generate each data point and the apparent corner on the initial 'transformation surface'. This test data together with the related surface morphology observations demonstrate the following distinct deformation features of the tube when the stress state changes from pure tension to pure torsion (via mixed loading): (1) both the transformation strain and the initial transformation stress exhibit strong anisotropy between tension and torsion; (2) there is a transition in the constitutive behavior of the material from instability under pure tension to stable deformation under pure shear; (3) correspondingly, as the loading path approaches the corner on the 'transformation surface', there is a gradual change in stress-induced transformation deformation mode, i.e., from the localization band initiation and propagation to homogeneous transformation, as shown by Figs. 7 and 8 and the surface morphology of the tube in Figs. 10 and 11.

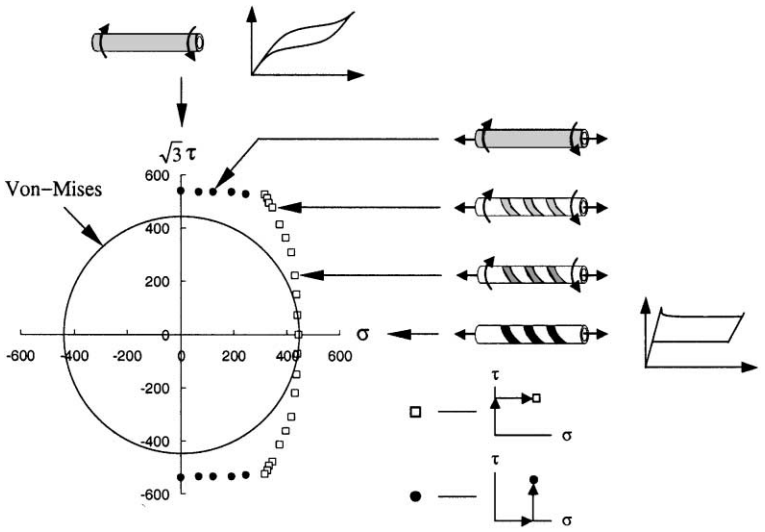

Fig. 9. Stress locus at the start of transformation: (□) tension under fixed torsion, (•) torsion under fixed tension.

4.4. Observation of the A–M interface thickness variation with stress state

The interface and the interface thickness play very important roles in the theory of first-order phase transitions in solids. To observe the variation in the A–M interface thickness during loading under an optical microscope, we designed and fabricated a special tension/torsion mini-loading frame. Different from the tests in Sections 4.2 and 4.3, here the tube is first put under tension in the axial direction until a spiral martensite band with sharp interfaces is nucleated as shown in the last photo (0°) in Fig. 10. Then, the displacement in the axial direction is fixed and torsion is applied by monotonically increasing the angle of rotation of the tube up to 138° (note: during torsion, the axial stress may change but it is not measured in the test). The corresponding total shear strain, γ, is about 4%. The measurement of the angle of rotation is quite satisfactory, with the error less than 1 degree. Fig. 10(a) shows the changes in the surface morphology of the tubes during the torsional loading process and Fig. 10(b) shows the corresponding unloading process. Fig. 10 shows that, with an increase in shear stress, the original sharp interface becomes more and more blurred (the interface sharpness is reduced due to an increase in the thickness of the interface). Since the tube material is superelastic, during unloading (removing the torsion while maintaining the tension), the previous sharp A–M interface gradually appears again due to the total recovery of the deformation produced during torsion and the final deformation returns back to the original tensile loading mode. Under high magnification, the changes in the interface thickness at the tube surface are shown in Fig. 11(a) (loading) and (b) (unloading). Fig. 11 shows that, unlike under uniaxial tension when the transformation deformation is realized by the move of sharp interfaces, during the above torsion, the A–M interface does not move but only broadens its extent. The relative distance between the interface and the triangle spot on the tube surface (marked by the white arrow in Fig. 11) remains unchanged. Quantitative measurement of the interface profile for biaxial loading is currently under way and will be reported in the future.

5. Discussion and concluding remarks

The experimental investigation reported in this paper on nano-grained polycrystalline NiTi microtubes reveals a strong constitutive anisotropy in both the kinetics and the kinematics of the material during

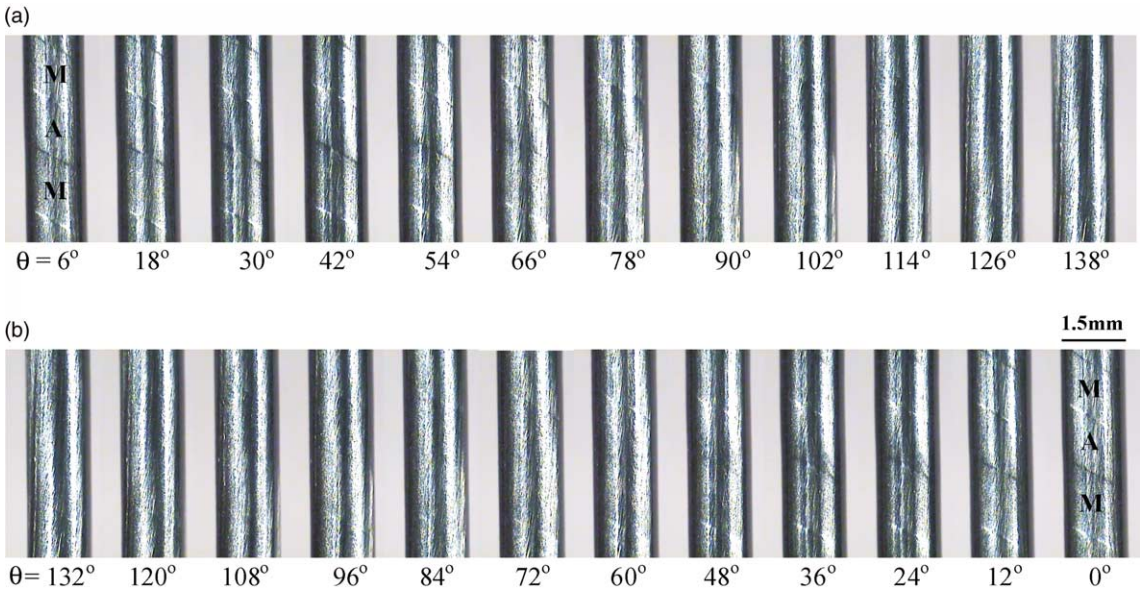

Fig. 10. The A–M interface thickness variation during (a) torsional loading and (b) unloading under fixed tensile loading (plateau stress).

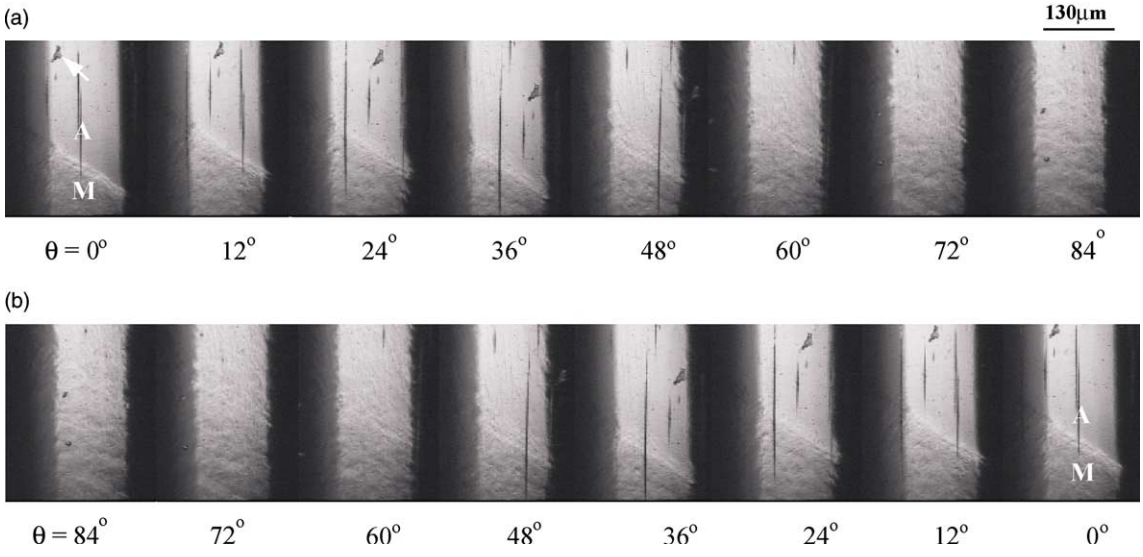

Fig. 11. Enlarged photos of the A–M interface evolution at tube surface (a) loading process (b) unloading process.

stress-induced transformation. Based on the biaxial tension/torsion test data and tube surface observations, the following preliminary conclusions are drawn:

- With uniaxial tensile loading along the tube axis direction, the stress-induced transformation deformation of superelastic polycrystalline NiTi SMA micro-tubes ($T > A_f$) is inhomogeneous and is realized by the initiation and growth of a spiral martensite band with a sharp A–M interface. As in previous inves-

tigations on superelastic NiTi wires and strips (Shaw and Kyriakides, 1995; Orgeas and Favier, 1998; Sun et al., 2000), it is again demonstrated that macroscopic deformation instability during stress-induced phase transformation exists for fine-grained NiTi micro-tubes under tensile loading conditions and the new phase generally has band morphology. Other common features of band nucleation and propagation have also been observed in micro-tube specimens. The initiation of the martensite band within a uniformly stressed region is accompanied by a stress drop, which is followed by a stress plateau in the subsequent band propagation. Inside the martensite band, the deformation is uniform and can be characterized by 'transformation strain' as measured using the high-resolution Moiré interference technique (Tse and Sun, 2000; Zhang et al., 2000). The martensite and austenite regions are separated by a narrow zone (macroscopic A–M interface) across which the strain changes very rapidly (Li and Sun, 2002).

- During loading by torsion (pure shear), the stress–strain curve exhibits monotonic hardening and the stress-induced transformation is axially homogeneous throughout the whole tube. This new observation together with the transformation strain and elastic modulus measurements reveal that there is a strong anisotropy in both the kinematics and the kinetics of the material's response during stress-induced transformation.
- Under tension–torsion combined loading, with an increasing shear/tension stress ratio, the deformation mode of the tube changes gradually from localization and propagation (under pure tension) to homogeneous deformation (under pure shear). This is clearly identified not only by the measured various stress–strain curves but also by the direct surface morphology observation. This gradual transition of deformation mode is accompanied by an increase in the A–M interface thickness. A strong loading path dependence of the deformation mode has been observed and a corner on the initial transformation surface has also been identified.

It has been well established that first-order martensitic phase transition is a typical instability phenomenon at the fundamental microscopic levels (such as non-convexity of free energy, non-monotonic stress–strain relations and interface structures). The essence of the science at this level has been well documented in the vast literature. The macroscopic constitutive description of a real NiTi polycrystal is, however, very different. This topic is still far from being fully understood and quantified. Instead of isotropic softening or hardening (see, for example, Sun and Hwang, 1993a,b), the preliminary work reported here has shown that the material may exhibit either stable (homogeneous) or unstable (inhomogeneous) deformation during transformation and that this strongly depends on both the internal microstructure (such as grain size, plastic deformation by dislocation, texture and heat treatment) and external loadings (such as stress state, loading history, temperature, loading rate, etc.). The understanding and modelling of the observed phenomena are of great significance in both academic research and the application of SMAs in the medical industry (such as in stent designs). A well-designed experimental study is crucial to such understanding. The anisotropic behavior described here strongly implies the very important effect of material microstructure in the deformation of real polycrystalline solids. The key question now remaining to be answered is what is the underlying physical mechanism/microstructure responsible for the observed anisotropy.

The strong initial texture due to the manufacturing process of the micro-tube specimen could be a possible mechanism for this anisotropic constitutive behavior. Zhao (1997) investigated the relationship between texture and anisotropy of shape memory properties. The results showed that, in as-rolled sheets, the tensile stress–strain curve has a clear plateau if the loading direction is along the rolling direction. In the case of loading along the transverse direction, the stress–strain curve does not show a plateau, and that further deformation requires an increase in the applied stress and an anisotropy in the behavior is therefore exhibited. Obviously, the effect of texture on the transformation behavior of micro-tubes and stents will be an important issue in the future studies. Another possible mechanism leading to macroscopic anisotropy

(such as in tension–compression and tension–torsion) may come directly from the intrinsic transformation anisotropy at the single crystal grain level. According to analysis by Sittner and Novak (2000), the macroscopic stress–strain deformation features of polycrystalline NiTi originate directly to the crystallography of the single crystals undergoing martensitic phase transformation. Sittner and Novak (2000) demonstrated that SMA polycrystals even with randomly oriented grains show tension/shear and tension/compression asymmetry in macroscopic stress–strain curves.

Many authors (Orgeas and Favier, 1998; Lim and McDowell, 1999; Gall and Sehitoglu, 1999; Liu et al., 1999) have found the asymmetries of transformation stress and transformation strain between tension and compression. Some have attributed the asymmetry to the low crystallographic symmetry of the martensite structure and the detwinning of the martensite in the deformation process of stress-induced martensite reorientation (Shu and Bhattacharya, 1998; Orgeas and Favier, 1998), whereas others (Gall and Sehitoglu, 1999; Thamburaja and Anand, 2001) have attributed the asymmetry to the texture. The effect of the stress state on the instability of the transformations, such as under tension, shear and compression, has not been systematically investigated. For example, the localized deformation mode (martensite band) under shear stress in polycrystalline NiTi (with or without texture) has not been observed so far in experiments (Orgeas and Favier, 1998) though band formation under tension has been well established. An in-plane shear test of a thin plate that exhibits transformation localization under tensile stress along all directions inside the plane (plane isotropic) was performed recently (Li, 2002). The preliminary results showed that a localized deformation mode did not exist under in-plane shear. Therefore another possible mechanism for the observed deformation instability under tension is the pure geometric effect which is not available in pure shear.

Acknowledgements

The authors are grateful for the financial support from the Research Grants Council of The Hong Kong SAR (Project no. HKUST6074/00E) and the National Natural Science Foundation of China (Project no. 19825107). The authors would like to thank Prof. R. Abeyaratne of MIT, Prof. J. Shaw of University of Michigan, Prof. S. Kyriakides of University of Texas and Prof. K. Bhattacharya of Caltech for stimulating discussions during the IUTAM Symposium. The authors also very much appreciate the two reviewers' comments in improving the paper. The Final-Year-Project undergraduate students Danial Fan and Wai-Ming Shing of the Mechanical Engineering Department of HKUST are acknowledged for their assistance in the testing and the surface morphology observations of the micro-tubes.

References

Abeyaratne, R., Knowles, J.K., 1990. On the driving traction acting on a surface of strain discontinuity in a continuum. J. Mech. Phys. Solids 38, 345–360.

Abeyaratne, R., Knowles, J.K., 1993. A continuum model of a thermoelastic solid capable of undergoing phase transitions. J. Mech. Phys. Solids 41, 541–571.

Duerig, T.W., 1995. Recent and future applications of shape memory and superelastic materials. Mater. Res. Soc. Symp. Proc. 360, 497–506.

Gall, K., Sehitoglu, H., 1999. The role of texture in tension–compression asymmetry in polycrystalline NiTi. Int. J. Plasticity 15, 69–92.

Li, Z.Q., Sun, Q.P., 2002. The initiation and growth of macroscopic martensite band in nano-grained NiTi microtube under uniaxial tension, Int. J. Plasticity, in press.

Li, Z.Q., 2002. Experimental investigation on phase transformation of superelastic NiTi microtubes, Ph.D. thesis. The Hong Kong University of Science and Technology, Hong Kong, China.

Liu, Y., Xie, Z.L., Van Humbeeck, J., Delaey, L., 1999. Effect of texture orientation on the martensite deformation of NiTi shape memory alloys sheet. Acta Mater. 47, 645–660.

Lim, T.J., McDowell, D.L., 1999. Mechanical behavior of an Ni–Ti shape memory alloy under axial-torsional proportional and nonproportional loading. ASME, J. Engng. Mater. Technol. 121, 9–18.

Miyazaki, S., No, V.H., Kitamura, K., Khantachawana, A., Hosoda, H., 2000. Texture of Ti–Ni rolled thin plates and sputter-deposited thin films. Int. J. Plasticity 16, 1135–1154.

Orgeas, L., Favier, D., 1998. Stress-induced martensitic transformation of a NiTi alloy in isothermal shear, tension and compression. Acta Mater. 46, 5579–5591.

Patoor, E., Niclaeys, C., Arbab Chirani, S., Ben Zineb, T., 2001. Influence of microstructural parameters on shape memory alloys behavior. In: Sun, Q.-P. (Ed.), Proceedings of the IUTAM Symposium on Mechanics of Martensitic Phase Transformation in Solids, June 11–15, Hong Kong. Kluwer Academic Publisher, New York.

Pelton, A. et al. (Eds.), 1997. Proceedings of the Second International Conference on Shape Memory and Superelastic Technologies (SMST-97), California, 2–6 March.

Shaw, J.A., Kyriakides, S., 1995. Thermomechanical aspects of NiTi. J. Mech. Phys. Solids 43, 1243–1281.

Shaw, J.A., Kyriakides, S., 1997. On the nucleation and propagation of phase transformation fronts in a NiTi alloy. Acta Mater. 45, 683–700.

Shu, Y., Bhattacharya, K., 1998. The influence of texture on the shape memory effect in polycrystals. Acta Mater. 46, 5457–5473.

Sittner, P., Novak, V., 2000. Anisotropy of martensitic transformations in modeling of shape memory alloy polycrystals. Int. J. Plasticity 16, 1243–1268.

Song, G.Q., Sun, Q.P., Hwang, K.C., 2000a. Effects of microstructure on the hardening and softening behavior of polycrystalline shape memory alloys. I. Micromechanics constitutive modelling. Acta Mecanica Sinica 16 (4), 309–324.

Song, G.Q., Sun, Q.P., Hwang, K.C., 2000b. Effects of microstructure on the hardening and softening behavior of polycrystalline shape memory alloys. II. Numerical simulation under axisymmetric loading. Acta Mecanica Sinica 16 (4), 325–334.

Sun, Q.P., Hwang, K.C., 1993a. Micromechanics modelling for the constitutive behavior of polycrystalline shape memory alloys. I. Derivation of general relations. J. Mech. Phys. Solids 41, 1–17.

Sun, Q.P., Hwang, K.C., 1993b. Micromechanics modelling for the constitutive behavior of polycrystalline shape memory alloys. II. Study of the individual phenomena. J. Mech. Phys. Solids 41, 19–33.

Sun, Q.P., Li, Z.Q., Tse, K.K., 2000. On superelastic deformation of NiTi shape memory alloy micro-tubes and wires—band nucleation and propagation. In: Gabbert, U., Tzou, H.S. (Eds.), Proceedings of IUTAM Symposium on Smart Structures and Structronic Systems. Kluwer Academic Publishers, Dordrecht, pp. 113–120.

Thamburaja, P., Anand, L., 2001. Polycrystalline shape-memory materials: effect of crystallographic texture. J. Mech. Phys. Solids 49, 709–737.

Tse, K.K., Sun, Q.P., 2000. Some deformation features of polycrystalline superelastic NiTi shape memory alloy thin strip and wire under tension. Key Eng. Mater. 177–180, 455–460.

Zhao, L., 1997. Texture development and anisotropic behaviour in a Ti–45Ni–5Cu (at.%) shape memory alloy. PhD thesis. University of Twente, Enschede, The Netherlands.

Zhang, X.Y., Sun, Q.P., Yu, S.W., 2000. A non-invariant plane model for the interface in Cu–Al–Ni single crystal shape memory alloys. J. Mech. Phys. Solids 48, 2163–2182.